Laser Acceleration of Relativistic Electrons Using the Inverse Cherenkov Effect

W. D. Kimura, G. H. Kim, R. D. Romea, and L. C. Steinhauer
STI Optronics, Inc., 2755 Northup Way, Bellevue, Washington 98004

I. V. Pogorelsky, K. P. Kusche, R. C. Fernow, and X. Wang
Brookhaven National Laboratory, ATF-Building 820, Upton, New York 11973

Y. Liu
Department of Physics, University of California, Los Angeles, California 90024
(Received 23 May 1994)

A 580-MW peak power, radially polarized CO_2 laser beam ($\lambda = 10.6\ \mu$m) focused by an axicon accelerated 40-MeV electrons by $\leq$3.7 MeV over a 12-cm interaction length (31 MeV/m), using the inverse Cherenkov effect in which a gas is used to slow the light wave. This represents the first direct observation of acceleration using this effect and demonstrates the effectiveness of the radially-polarized–axicon-focused geometry. The observed energy gain agrees with model predictions.

PACS numbers: 41.75.Ht, 29.17.+w, 42.62.Hk

Using lasers to accelerate relativistic particles [1] offers the potential for generating >1 GeV/m acceleration gradients, thereby enabling the possibility of TeV-class (10^{12} eV) accelerators and compact accelerators for use in industry and medicine. This Letter presents the experimental results of using the inverse Cherenkov effect to accelerate electrons in which a gas (e.g., H_2) is used to slow the phase velocity of the laser light to match the electron velocity [2]. Phase matching is achieved by intersecting the laser light with the electron beam (e beam) at the Cherenkov angle defined by $\theta_C = \cos^{-1}(1/n\beta)$, where n is the index of refraction of the gas and β is the electron velocity divided by the velocity of light. Satisfying the Cherenkov phase matching condition enables electrons to stay in phase with the light wave over long distances resulting in large accumulated energy gains.

The inverse Cherenkov effect was first demonstrated at Stanford University in 1981 [2]. Later, Fontana and Pantell [3] developed an improved geometry for inverse Cherenkov acceleration (ICA) that features a radially polarized laser beam focused onto the e beam using an axicon (see Fig. 1). This geometry offers several advantages over the linearly polarized laser beam case, including more efficient energy exchange, and is the one used in the experiment discussed here.

The experiment was performed on the Accelerator Test Facility (ATF) at Brookhaven National Laboratory [4]. The ATF features a 40-MeV electron accelerator that uses a photocathode microwave e gun. A 10-GW linearly polarized CO_2 laser ($\lambda = 10.6\ \mu$m) is available for laser particle acceleration experiments [5].

The major components of the experiment are an optical system for converting the linearly polarized ATF CO_2 laser beam into one with radial polarization [6], a gas cell where the ICA interaction occurs, and an e-beam transport line and energy spectrometer. Figure 2 is a schematic plan view of the gas cell. The electrons enter through a 2.1-μm-thick diamond window, which separates the gas in the cell from the beam-line vacuum, travel through a 0.5-mm diam hole in the axicon mirror, pass through the interaction region and a 1-mm diam hole in a 45° mirror, exit the cell through another 2.1-μm-thick diamond window, and continue to the energy spectrometer at the end of the beam line. Entering the cell through a ZnSe window, the radially polarized laser beam reflects off the 45° mirror towards the axicon mirror, which focuses the laser beam onto the e beam.

The axicon had a measured angle of 10.04 ± 0.04 mrad, corresponding to a Cherenkov angle under ideal conditions of 20.08 ± 0.08 mrad. The laser beam on the axicon had an estimated outer radius of ~3.75 mm and an inner radius of ~1.25 mm (90% power points). This meant the interaction length was ≈12 cm.

The amount of laser power that could be delivered during the experiment was limited by laser damage of one of the optical elements in the system. Although this situation was rectified after the experiment, it meant the

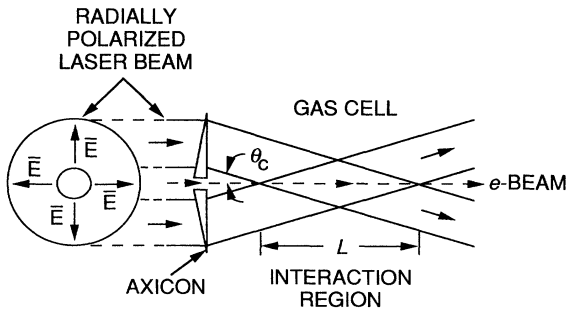

FIG. 1. Inverse Cherenkov acceleration configuration [3]. A radially polarized laser beam is focused by an axicon onto the e beam at the Cherenkov angle θ_C inside a gas-filled region, resulting in energy exchange occurring over an interaction length L.

 0031-9007/95/74(4)/546(4)$06.00

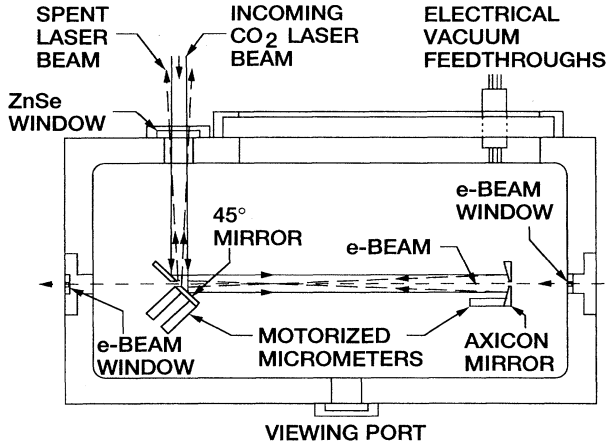

FIG. 2. Schematic plan view of the gas cell where the inverse Cherenkov interaction occurs. Note that an axicon mirror is used rather than an axicon lens, as shown in Fig. 1. The optics in the gas cell can be adjusted remotely.

effective peak power delivered to the interaction region was ~580 MW. This effective power includes a correction factor because the delivered laser beam was also only 83% radially polarized. (Normally this is >90%.) The parameters for the experiment are summarized in Table I.

The energy spectrometer has a momentum acceptance range of ±2.8% of the mean energy. Since the ICA interaction resulted in an energy modulation much larger than this range, it was necessary to scan the spectrometer and use multiple shots to obtain subspectra in order to construct the full modulated spectrum.

TABLE I. Experiment system parameters.

Electron beam	
Source	BNL ATF
Beam energy	40 MeV
Intrinsic energy spread (σ)	$\approx\pm 0.5$ MeV
Normalized emittance[a]	$\sim 20\pi$ mm mrad
Electron bunch length	$\approx$13 ps (FWHM)
Charge per bunch	$\approx$0.1 nC
Pulse format	Single pulse
Laser beam	
Laser	CO_2
Wavelength	10.6 μm
Pulse length (base width)	220 ps
Peak power delivered to interaction region	~580 MW
Pulse repetition rate	Single shot
Interaction region (gas cell)	
Phase matching medium	Hydrogen gas
Cherenkov angle	20.08 ± 0.08 mrad
Temperature	16.7 °C
Length of electron/laser beam overlap	$\approx$12 cm
Length of gas traversed by electrons	43 cm
Thickness of diamond e-beam window	2.1 μm

[a]Effective geometric emittance as defined by the limiting apertures inside the gas cell.

Some pulse-to-pulse changes in the e-beam and laser beam characteristics occurred during the scan. The largest fluctuations were in the e-beam current ($\sigma \approx 50\%$), which only changed the magnitude of the spectrometer signal and not the overall shape of the full spectrum. Instabilities of the mean e-beam energy due to RF power fluctuations add a $\approx\pm 93$ keV uncertainty in the energy values of the full spectrum, but, as will be shown, this is much less than the acceleration imparted upon the e beam by the laser. Last, the laser pulse energy varied with a $\sigma \approx 14\%$; however, since the ICA interaction scales with the square root of the laser peak power [3], this amount of variation does not appreciably change the shape of the full spectrum. Thus, even though the conditions are not exactly the same for each of the subspectra, an approximate full spectrum can be created by scaling the subspectra to fit end to end to compensate for the variations in e-beam current [7].

Figure 3(a) gives the e-beam energy spectrum after traversing through the gas cell filled with 2.2 atm of H_2 at 16.7 °C, with the laser off. Most of the energy spread is due to the intrinsic width of the e beam ($\sigma \approx 0.5$ MeV). Figure 3(b) shows the result with the laser delivering ~580 MW, where the subspectra have been spliced together. Since the electron bunch length ($\tau/c \sim 4$ mm) is much longer than the laser wavelength, the interaction between the e beam and the laser beam occurred over all phases of the laser light wave, resulting in both accelerated and decelerated electrons being observed. These data, taken at a constant spectrometer detector gain, show a maximum acceleration of ~3 MeV; however, as will be shown later, electrons were accelerated beyond 3 MeV.

The predictions of the model developed to simulate the ICA process [8], which includes the effects of electron scattering by the gas molecules, are also plotted in Fig. 3. In Fig. 3(a), the model and data are in excellent agreement. Two slightly different model runs are given in Fig. 3(b) where the gas cell exit window diameter is either 1 or 2 mm, with the 1-mm case being closer to the actual size of the output window. The model predicts that as the output window size decreases more electrons are accelerated or decelerated relative to the unaccelerated ones. (Note that the ordinate in Fig. 3 is normalized to the peak signal and does reveal the fact that the overall signal is lower for a smaller window.) The interpretation of this is that the output window acts like a filter to the spectrometer by controlling the number of off-axis electrons that are detected versus the number of on-axis electrons. It is the on-axis electrons that in general will experience the best energy exchange. Therefore, the smaller the output window, the fewer unaccelerated electrons are detected, which after normalization of the spectra makes it appear that relatively more electrons are

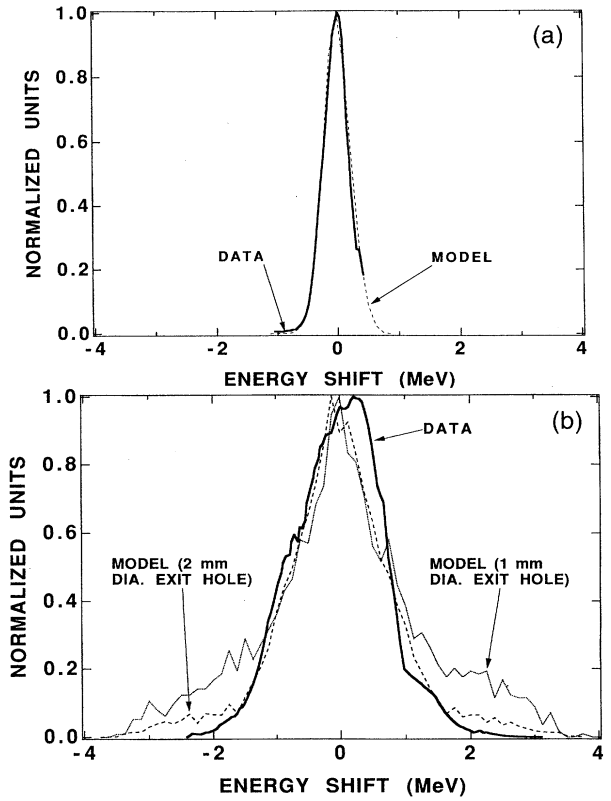

FIG. 3. Electron-beam energy spectra. Solid curves are the subspectra data that have been spliced together (see text), dashed and dotted curves are the model predictions [8]. (a) With no laser present and after traveling through the gas cell filled with 2.2 atm H_2 at 16.7 °C. (b) With 580 MW of laser peak power delivered to the interaction region and measured at constant spectrometer detector gain.

accelerated. This behavior implies that the model may need to be modified to include other effects such as a nonuniform laser beam wave front that can cause less efficient energy exchange.

Electrons at ~3.7 MeV are seen in the subspectra obtained at the highest spectrometer detector gain (see Fig. 4) and correspond to an acceleration gradient of ≈31 MeV/m. (Note, the number of electrons gaining high energy can be increased by optically prebunching the e beam before it interacts with the laser accelerator.)

At 580-MW laser peak power, theory predicts the maximum longitudinal electric field at the optimum phase point is 3.5×10^5 V/cm, corresponding to a peak acceleration gradient of 35 MeV/m. This is consistent with the measured average gradient of 31 MeV/m.

The pressure was varied to optimize the interaction and, based upon the optimum pressure point, to determine the effective Cherenkov angle of the experiment. Figure 5 shows the measured and predicted pressure dependence of the ICA process. The model predictions for the peak

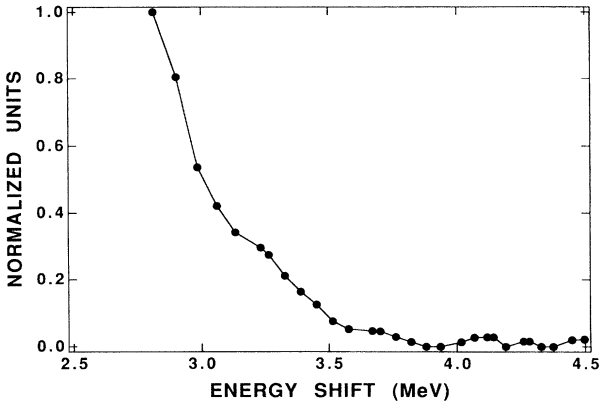

FIG. 4. Electron-beam energy subspectrum (single shot data) of the high energy region obtained with the spectrometer detector set to maximum gain. All the other conditions are the same as in Fig. 3.

acceleration as a function of gas pressure are plotted. Because of the pulse-to-pulse variations explained earlier, the peak acceleration of the data as a function of pressure could not be reliably measured. Instead, Fig. 5 plots the width of the normalized central subspectrum (at 80% of the peak) versus pressure. This is a less direct method for determining the pressure dependence of the electron modulation by the laser since it measures the change in shape of only a small portion of the full spectrum [9]. As seen in Fig. 3, the central portion of the laser-on spectrum is slightly wider than the laser-off spectrum. However, the limited momentum acceptance of the spectrometer will also tend to mask this spreading effect. Therefore, it is not expected that the shapes of the model and data pressure dependence curves would necessarily agree with each other. Nonetheless, it is useful to note that the maximum for the data occurs at a slightly lower gas

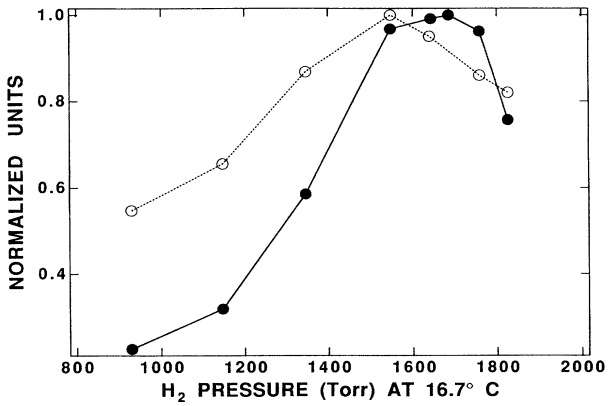

FIG. 5. Gas pressure dependence results. The solid curve is the model prediction, where the normalized maximum electron acceleration is plotted as a function of pressure. The dashed curve is the data, where the normalized width of the measured central subspectrum is plotted as a function of pressure.

pressure than the model prediction and corresponds to a Cherenkov angle of ~19.4 mrad. This may be due to an imperfectly collimated laser beam at the axicon. The more gradual pressure dependence of the data is also consistent with the spectrometer's limited acceptance range tending to mask the spreading effect.

Current detector limitations [7] prevented the number of electrons accelerated to higher energies from being quantified during this particular experiment. However, a strong spectrometer signal was obtained which indicated that a significant fraction of the total number of electrons in the e-beam pulse was being accelerated with each shot. Based upon the sensitivity of the spectrometer detector system, we estimate that the spectrum shown in Fig. 3(b) corresponds to roughly 10 pC of charge. Since the data are in good agreement with the model, we can use this total charge value and the shape of the model curve to estimate that $>10^6$ electrons received energy gains >2 MeV.

The strong spectrometer signal also provided a convenient way to determine the timing between the electron pulse (~13 ps) and the laser pulse, and to optimize the spatial overlap between the two beams within the interaction region. By scanning the delay time between the two beams and observing the spectrometer signal of the accelerated electrons, the duration of the laser pulse was measured and found to be 220 ps (base width). This ease in controlling the timing implies that synchronizing the e-beam pulse with shorter length laser pulses (e.g., 30 ps) should not be an issue for future experiments.

In conclusion, an electron energy gain of ≤3.7 MeV using the inverse Cherenkov effect was observed, in good agreement with the model predictions. This is the highest amount of acceleration observed for this effect. This demonstration validates the improved ICA geometry devised by Fontana and Pantell. Future plans include performing additional ICA measurements at higher delivered laser peak power (~5 GW) and for longer interaction lengths (~20 cm). Under these conditions the model predicts >12 MeV peak acceleration representing an acceleration gradient of >60 MeV/m. Upgrading the ATF CO_2 laser to generate >100 GW of peak power would enable acceleration gradients of several hundred MeV per meter.

The authors wish to acknowledge Dr. J. R. Fontana, Dr. R. H. Pantell, and Dr. I. Ben-Zvi for their helpful discussions, and Dr. A. S. Fisher, M. Babzien, K. Batchelor, and Dr. T. Srinivasan-Rao for their valuable assistance during the experiment. This work was supported by the U.S. Department of Energy, Grant No. DE-FG06-93ER40803.

[1] A. M. Sessler, Am. J. Phys. **54**, 505 (1986).
[2] J. A. Edighoffer, W. D. Kimura, R. H. Pantell, M. A. Piestrup, and D. Y. Wang, Phys. Rev. A **23**, 1848 (1981).
[3] J. R. Fontana and R. H. Pantell, J. Appl. Phys. **53**, 5435 (1982).
[4] I. Ben-Zvi, in *Advanced Accelerator Concepts,* edited by J. S. Wurtele, AIP Conf. Proc. No. 279 (AIP, New York, 1993), p. 590.
[5] I. Pogorelsky, in *Advanced Accelerator Concepts* (Ref. [4]), p. 608.
[6] S. C. Tidwell, G. H. Kim, and W. D. Kimura, Appl. Optics **32**, 5222–5229 (1993).
[7] A Faraday cup was positioned at the output end of the spectrometer for measuring the e-beam current; however, it was limited by noise during the experiment. This limitation also prevented using this sensor for monitoring fluctuations in the e-beam current.
[8] R. D. Romea and W. D. Kimura, Phys. Rev. D **42**, 1807–1818 (1990).
[9] Although in principle the model prediction for the width of the central portion of the spectrum could be compared with the width of the central subspectrum data, the accuracy of this comparison is constrained by limitations in the accuracy of the spectrometer momentum acceptance calibration.